

Annular Electroconvection with Shear

Zahir A. Daya,¹ V. B. Deyirmenjian,¹ Stephen W. Morris,¹ and John R. de Bruyn²

¹*Department of Physics and Erindale College, University of Toronto, 60 St. George Street, Toronto, Ontario, Canada M5S 1A7*

²*Department of Physics and Physical Oceanography, Memorial University of Newfoundland, St. John's, Newfoundland, Canada A1B 3X7*

(Received 9 October 1997)

We report experiments on convection driven by a radial electrical force in suspended annular smectic-*A* liquid crystal films. In the absence of an externally imposed azimuthal shear, a stationary 1D pattern consisting of symmetric vortex pairs is formed via a supercritical transition at the onset of convection. Shearing reduces the symmetries of the base state and produces a traveling 1D pattern whose basic periodic unit is a pair of asymmetric vortices. For a sufficiently large shear, the primary bifurcation changes from supercritical to subcritical. We describe measurements of the resulting hysteresis as a function of the shear at radius ratio $\eta \sim 0.8$. [S0031-9007(97)05181-8]

PACS numbers: 47.20.Ky, 47.54.+r

Extended nonlinear dissipative systems can develop complicated spatial and temporal patterns when subjected to external stresses by the variation of a control parameter [1]. The observed patterns are often the result of symmetry-breaking bifurcations. In some cases, additional control parameters can alter the symmetries of the base state which in turn affects the bifurcation to the patterned state. For example, in a large cylinder, the onset of Rayleigh-Bénard convection (RBC) is stationary. However, rotating the cylinder breaks the reflection symmetry in any vertical plane containing the rotation axis, and convection occurs via a Hopf bifurcation [2]. Varying the rotation rate can move the system into a regime of spatiotemporal chaos [3]. It is useful to identify other simple situations in which pattern forming bifurcations can be “tuned” by additional control parameters in order to better understand how we can manipulate spatiotemporal patterns.

In this Letter, we exploit the novel properties of electroconvection in freely suspended smectic-*A* liquid crystal films in an annular geometry to study how azimuthal shear affects pattern formation. This is accomplished by measuring the current-voltage characteristics of films subjected to a dc voltage between the inner and outer edges of the annulus. A variable Couette shear is applied by rotating the inner edge of the annulus. The films had a radius ratio $\eta = r_i/r_o \sim 0.8$, where r_i (r_o) is the inner (outer) radius. For zero shear, a stationary one-dimensional (1D) pattern, consisting of pairs of symmetric vortices, appears via a continuous bifurcation at a voltage V_c^0 . For nonzero shear, an azimuthally traveling 1D pattern, whose basic unit is a pair of unequally sized vortices, is established. When the shear is of sufficient magnitude, the primary bifurcation becomes discontinuous. The combination of applied shear, radial electrical driving forces, and a two-dimensional (2D) annular geometry makes it possible to adjust the symmetries of the base state and the nature of the primary bifurcation.

Electroconvection in suspended smectic films without applied shears has been the subject of several previous experimental and theoretical studies [4–12]. Smectic liquid crystals are materials which consist of layers of orientationally ordered molecules. In smectic *A*, the long axis of the molecules is normal to the layer plane. In this arrangement, smectic *A* exhibits 2D isotropic fluid properties in the layer plane, and flow normal to the layers is strongly suppressed [4–8]. Finite rectangular smectic-*A* films were the subject of previous experimental work [4–8], while the linear and weakly nonlinear theories have been completed for the case of a 2D weakly conducting fluid in a laterally unbounded rectangular geometry [9,10]. Convection has also been studied in smectic-*C* films in which the molecular axes are tilted with respect to the layer normal and can be reoriented by the flow [11,12]. These anisotropic effects will not concern us here.

There are several features of this system which distinguish it from the well-studied cases of RBC and Taylor vortex flow (TVF). The 2D nature of the flow severely restricts the secondary instabilities available to the pattern [7]. A Couette shear flow cannot easily be superposed on RBC as is accomplished in annular electroconvection. This is also one of a handful of pattern forming systems in which the dynamics are governed by interactions mediated by long range forces. The forces driving convection result from the interaction between the electric field and a nonzero surface charge density on the film [9,10]. The relation between the surface charge density and the electric field is nonlocal, i.e., the charge density at any point on the film depends on the electric field everywhere, which gives rise to a long range coupling between different parts of the pattern.

An additional consequence of the shear is the imposition of an azimuthal mean flow. RBC with horizontal mean flow and TVF with axial mean flow have been investigated experimentally and theoretically [1,13–15].

These open flow studies showed that the first instability is *convective*, i.e., that localized perturbations grow as they are advected downstream, but decay at the point of initiation. At higher control parameter, the instability becomes *absolute*, so that localized perturbations grow at the point of initiation. In both cases, the pattern drifts in the direction of the mean flow. In contrast, our annular system is a closed flow, so that an advected perturbation returns to its starting point. At present, our experiments do not distinguish between convective and absolute instability. It is also interesting to note that, unlike in 3D TVF, an imposed Couette shear flow alone does not lead to an instability in a 2D fluid [16]. We show below that these shears always have the effect of suppressing electroconvection.

This system also possesses interesting symmetries. In the absence of shear, the base state is invariant under azimuthal rotation and reflection in any vertical plane containing the rotation axis through the center of the annulus. The application of azimuthal shear breaks the latter reflection symmetry and distinguishes between the clockwise and counterclockwise directions. This results in a pattern at the onset of electroconvection which travels in the direction of the mean flow.

Our experimental apparatus consisted of two stainless steel electrodes. The inner electrode was a circular disk of diameter 8.96 ± 0.01 mm. The outer electrode was a larger circular plate with a central hole of diameter 11.20 ± 0.01 mm. The annular film was suspended between the concentric inner and outer electrodes, giving a radius ratio $\eta = 0.800 \pm 0.001$. A motorized stainless steel blade wetted with liquid crystal was slowly drawn across the annulus to form a film. This procedure allowed for the drawing of uniform films of various thicknesses. The films were composed of integer numbers of smectic layers. Each layer of smectic-A 8CB [17] is 3.16 nm thick. The experiments employed films of up to 75 layers. The films were viewed through a microscope with a color video camera. When viewed in reflected white light, the films displayed a color due to interference. By visually monitoring the film color throughout each experiment, we confirmed that the films had a constant thickness over their whole area which remained uniform to within ± 1 layer. The inner electrode was rotated about its axis by a high precision stepper motor at angular frequencies up to $\omega \sim 10$ rad/s. All experiments were performed at 23 ± 1 °C, well below the smectic-A–nematic transition at 33 °C for pure 8CB. The system was shielded by a Faraday cage, and the outer electrode and shield were maintained at ground potential while the voltage of the inner electrode was varied above ground. The resulting current through the film was measured using a picoammeter.

A plot of a typical current-voltage response in the absence of shear is shown in Fig. 1(a). These data were obtained by slowly increasing and then decreasing the applied voltage in small steps. After each voltage step,

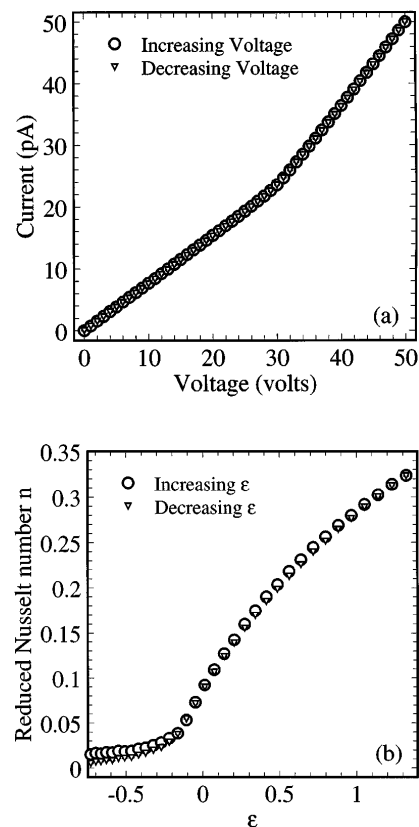


FIG. 1. (a) The current-voltage measurements for an annular film with radius ratio $\eta \sim 0.8$. (b) The reduced Nusselt number n vs the control parameter ϵ .

the film was allowed to relax for about 10 s, before 20–25 measurements of the current, each separated by 250 ms, were averaged. The film behaved as an Ohmic conductor in the conduction regime below the onset of electroconvection. At a critical voltage V_c^0 , the film was unstable to a stationary vortex pattern which broke the continuous axisymmetry of the base state. The fluid flow could be visualized by allowing fine dust to settle on the film. The pattern was comprised of pairs of equally sized, symmetric, counterrotating vortices. V_c^0 was identified by the position of the kink in the current-voltage response [see Fig. 1(a)]. No hysteresis in the onset was observed between runs with increasing and decreasing voltage. These data are similar to those found previously for rectangular films, but are much more precise, since annular films do not suffer from the problem of leakage of current around the ends of the film [6].

In analogy with the convective heat transport in RBC, we describe the dimensionless convective current by a reduced Nusselt number $n = I/I_c - 1$, where I (I_c) is the total (conductive) current. The dimensionless control parameter for this system is [9,10] $\mathcal{R} = \epsilon_0^2 V^2 / \sigma \mu s^2$, where ϵ_0 is the dielectric constant of free space, σ is the bulk conductivity, μ is the bulk molecular viscosity, and s is the film thickness. We employ the reduced control

parameter $\epsilon = \mathcal{R}/\mathcal{R}_c^0 - 1 = (V/V_c^0)^2 - 1$. When recast in terms of n and ϵ , the current-voltage data take the form shown in Fig. 1(b), which is typical of a supercritical bifurcation [18].

The number of vortex pairs that is generated in the unsheared annulus equals the number that would appear in a rectangular film whose length equals the circumference of the annulus [5]. We expect, however, the range of stable vortex wavelengths in the annulus will be different from the rectangular case. In the latter, the range is determined by the boundary conditions at the ends of the film [7]. In the annulus, the 1D pattern is effectively subject to periodic boundary conditions.

When the inner electrode is rotated about its axis, the film is subjected to a steady shear. The sheared film was allowed about 30 s to attain a steady state, after which current-voltage data were acquired as described earlier. Figure 2(a) compares the current-voltage characteristic for the same film when the base state is quiescent or sheared. For small shears, the onset of convection occurs by a continuous transition and is identified by a kink in the current-voltage data, as in the zero shear case. When the shear is sufficiently large, the transition is subcritical and discontinuous and is revealed by a jump in the current. In

this regime, the bifurcation is hysteretic with convection appearing at $V_c^+(\omega)$ as V is increased, and disappearing at $V_c^-(\omega)$ as V is decreased. The onset of convection is suppressed by the shear as $V_c^\pm(\omega) > V_c^0$.

Figure 2(b) is a plot of n versus $\tilde{\epsilon} = \mathcal{R}(\omega)/\mathcal{R}_c^0 - 1 = [V(\omega)/V_c^0]^2 - 1$ for a sheared film. The transition from the conducting (convecting) state to the convecting (conducting) state occurs at $\tilde{\epsilon}_+$ ($\tilde{\epsilon}_-$), where $\tilde{\epsilon}_\pm = [V_c^\pm(\omega)/V_c^0]^2 - 1$. The hysteresis, $\delta\tilde{\epsilon} = \tilde{\epsilon}_+ - \tilde{\epsilon}_-$, is shear dependent. We nondimensionalize the rotation rate by the charge relaxation time characteristic of the annular film [6,9,10], $\tau = \epsilon_0(r_o - r_i)/\sigma s$. From the current-voltage characteristic of the film in the conduction regime, the product $\sigma s = \ln(r_o/r_i)/2\pi\rho$, where ρ is the film resistance. We therefore define the dimensionless angular frequency as $\tilde{\omega} = 2\pi\omega\epsilon_0(r_o - r_i)\rho/\ln(r_o/r_i)$. Our results for $\delta\tilde{\epsilon}$ in eleven experiments at various $\tilde{\omega}$ are plotted in Fig. 3(a). For $\tilde{\omega} \lesssim 1.7$, the hysteresis is consistent with zero which indicates that the bifurcation is continuous for small shears. In Fig. 3(b) are shown measurements of $\tilde{\epsilon}_+$ and $\tilde{\epsilon}_-$. We find that there is strong suppression of convection by the shear, with $\tilde{\epsilon}_+ > 7$ for the largest $\tilde{\omega}$ studied.

The traveling pattern in the sheared experiment is most simply described in a frame that rotates at the angular speed at which the pattern appears stationary. In this frame it consists of a periodic array of vortex pairs. Each pair

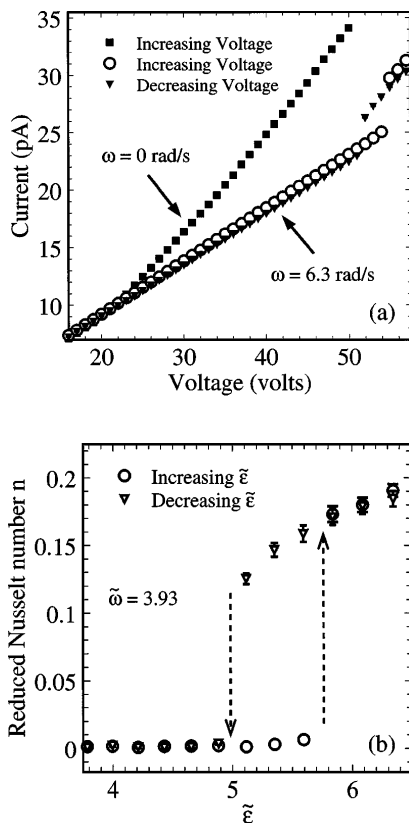


FIG. 2. (a) The current-voltage measurements for the same film with and without applied shear. (b) The reduced Nusselt number n vs $\tilde{\epsilon}$ for a film sheared at dimensionless angular frequency $\tilde{\omega} = 3.93$.

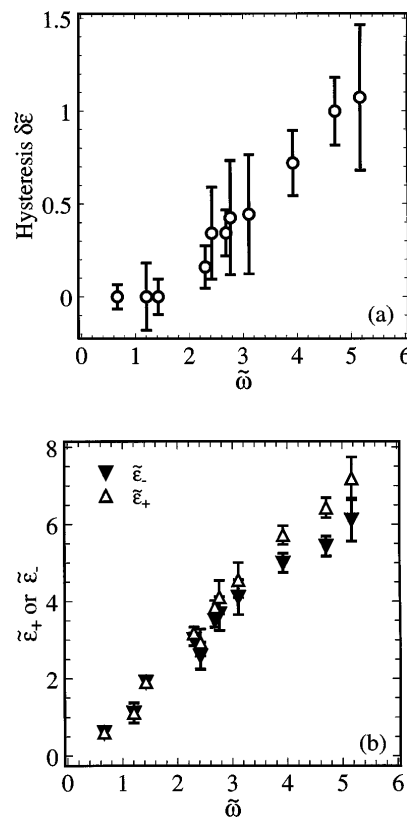


FIG. 3. (a) Hysteresis $\delta\tilde{\epsilon}$ vs the dimensionless angular frequency $\tilde{\omega}$. (b) Measurements of $\tilde{\epsilon}_+$ and $\tilde{\epsilon}_-$ vs $\tilde{\omega}$.

is asymmetric, composed of counterrotating vortices of unequal width. The vortex whose circulation is in the same direction as the rotation of the inner electrode is narrower while the opposite sense vortex is broader. The number of traveling vortices observed depends hysteretically on $\tilde{\epsilon}$ and $\tilde{\omega}$ and is generally smaller than in the unsheared case. Transitions between different numbers of vortices can be observed as $\tilde{\epsilon}$ and $\tilde{\omega}$ are varied. The sheared base state is invariant under azimuthal rotations, but not under reflections. The onset of convection breaks the azimuthal symmetry, and the resulting traveling pattern has no continuous spatial symmetries.

In summary, we measured the current-voltage characteristics of radially driven electroconvection in freely suspended annular smectic-A films under varying degrees of azimuthal shear. Shearing, which was generated by rotating the inner edge of the annulus at an angular frequency $\tilde{\omega}$, altered the symmetries of the system and changed the primary bifurcation from stationary, when $\tilde{\omega} = 0$, to oscillatory. Adjusting $\tilde{\omega}$ allowed us to tune the primary symmetry-breaking bifurcation and suppress the onset of convection. Without shear, the onset of electroconvection was supercritical, but the transition became subcritical with a large enough shear. The pattern consisted of symmetric (asymmetric) vortex pairs when $\tilde{\omega} = 0$ ($\tilde{\omega} \neq 0$). Future work on this system will involve an experimental study of the secondary instabilities of the pattern. It is also interesting to explore the effect of smaller radius ratios. This pattern forming instability should be simple enough to be captured by a quantitative nonlinear theory.

We are grateful to T.C.A. Molteno, W.A. Tokaruk, K. Choo, W. Langford, and M. Krupa for helpful discussions and assistance during the course of this work. This research was supported by the Natural Sciences and Engineering Research Council of Canada.

[1] M.C. Cross and P.C. Hohenberg, *Rev. Mod. Phys.* **65**, 851 (1993).

[2] F. Zhong, R.E. Ecke, and V. Steinberg, *Phys. Rev. Lett.* **67**, 2473 (1991); R.E. Ecke, F. Zhong, and E. Knobloch,

Europhys. Lett. **19**, 177 (1992); E. Knobloch, in *Lectures on Solar and Planetary Dynamos*, edited by M.R.E. Proctor and A.D. Gilbert (Cambridge University Press, New York, 1994), p. 331.

- [3] M. van Hecke and W. van Saarloos, *Phys. Rev. E* **55**, R1259 (1997).
- [4] S.W. Morris, J.R. de Bruyn, and A.D. May, *Phys. Rev. Lett.* **65**, 2378 (1990).
- [5] S.W. Morris, J.R. de Bruyn, and A.D. May, *J. Stat. Phys.* **64**, 1025 (1991).
- [6] S.W. Morris, J.R. de Bruyn, and A.D. May, *Phys. Rev. A* **44**, 8146 (1991).
- [7] S.S. Mao, J.R. de Bruyn, Z.A. Daya, and S.W. Morris, *Phys. Rev. E* **54**, R1048 (1996).
- [8] S.S. Mao, J.R. de Bruyn, and S.W. Morris, *Physica (Amsterdam)* **239A**, 189 (1997).
- [9] Z.A. Daya, S.W. Morris, and J.R. de Bruyn, *Phys. Rev. E* **55**, 2682 (1997).
- [10] V.B. Deyirmenjian, Z.A. Daya, and S.W. Morris, *Phys. Rev. E* **56**, 1706 (1997).
- [11] S. Ried, H. Pleiner, W. Zimmermann, and H.R. Brand, *Phys. Rev. E* **53**, 6101 (1996).
- [12] A. Becker, S. Ried, R. Stannarius, and H. Stegemeyer, *Europhys. Lett.* **39**, 257 (1997).
- [13] K.L. Babcock, G. Ahlers, and D.S. Cannell, *Phys. Rev. E* **50**, 3670 (1994).
- [14] H.W. Muller and M. Tveitereid, *Phys. Rev. Lett.* **74**, 1582 (1995).
- [15] S.P. Trainoff, D.S. Cannell, and G. Ahlers (unpublished); S.P. Trainoff, Ph.D. thesis, University of California, Santa Barbara, 1997 (unpublished).
- [16] X.-I. Wu, B. Martin, H. Kellay, and W.I. Goldburg, *Phys. Rev. Lett.* **75**, 236 (1995).
- [17] To control the nature of the ionic species in the liquid crystal, octylcyanobiphenyl (8CB) was doped with tetracyanoquinodimethane (TCNQ).
- [18] The difference between the data for increasing and decreasing ϵ , which is evident in Fig. 1(a) for $\epsilon < -0.25$, is a consequence of a downward drift in the conductivity of the film over the course of the experiment. This drift was typically 2% over the course of a run, and is due to electrochemical reactions between the liquid crystal and the electrodes. See S. Barret, F. Gaspard, R. Herino, and F. Mondon, *J. Appl. Phys.* **47**, 2375 (1976).